Seduction of Finding Universality in Sputtering Yields Due to Cluster Bombardment of Solids

ARTICLE *in* ACCOUNTS OF CHEMICAL RESEARCH · AUGUST 2015

Impact Factor: 22.32 · DOI: 10.1021/acs.accounts.5b00303

3 AUTHORS:

Robert J Paruch
Pennsylvania State University
28 PUBLICATIONS **193** CITATIONS
SEE PROFILE

Zbigniew Postawa
Jagiellonian University
137 PUBLICATIONS **1,936** CITATIONS
SEE PROFILE

Barbara Garrison
Pennsylvania State University
368 PUBLICATIONS **9,348** CITATIONS
SEE PROFILE

ACCOUNTS of chemical research

Article

pubs.acs.org/accounts

Seduction of Finding Universality in Sputtering Yields Due to Cluster Bombardment of Solids

Robert J. Paruch,*[,†] Zbigniew Postawa,[‡] and Barbara J. Garrison[†]

[†]Department of Chemistry, Penn State University, 104 Chemistry Building, University Park, Pennsylvania 16802, United States

[‡]Smoluchowski Institute of Physics, Jagiellonian University, ulica Lojasiewicza 11, 30-348 Krakow, Poland

Supporting Information

CONSPECTUS: Universal descriptions are appealing because they simplify the description of different (but similar) physical systems, allow the determination of general properties, and have practical applications. Recently, the concept of universality has been applied to the dependence of the sputtering (ejection) yield due to energetic cluster bombardment versus the energy of the incident cluster. It was observed that the spread in data points can be reduced if the yield Y and initial projectile cluster kinetic energy E are expressed in quantities scaled by the number of cluster atoms n, that is, Y/n versus E/n. The convergence of the data points is, however, not perfect, especially when the results for molecular and atomic solids are compared. In addition, the physics underlying the apparent universal dependence in not fully understood. For the study presented in this Account, we performed molecular dynamics simulations of Ar_n cluster bombardment of molecular (benzene, octane, and β-carotene) and atomic (Ag) solids in order to address the physical basis of the apparent universal dependence. We have demonstrated that the convergence of the data points between molecular and atomic solids can be improved if the binding energy of the solid U_0 is included and the dependence is presented as $Y/(E/U_0)$ versus $(E/U_0)/n$. As a material property, the quantity U_0 is defined per the basic unit of material, which is an atom for atomic solids and a molecule for molecular solids. Analogously, the quantity Y is given in atoms and molecules, respectively. The simulations show that, for almost 3 orders of magnitude variation of $(E/U_0)/n$, there are obvious similarities in the ejection mechanisms between the molecular and atomic solids, thus supporting the concept of universality. For large $(E/U_0)/n$ values, the mechanism of ejection is the fluid flow from a cone-shaped volume. This regime of $(E/U_0)/n$ is generally accessed experimentally by clusters with hundreds of atoms and results in the largest yields. For molecular systems, a large fraction of the total energy E is consumed by internal excitation and molecular fragmentation, which are energy loss channels not present in atomic solids. For small $(E/U_0)/n$ values, the cluster deforms the surface and the ejection occurs from a ring-shaped ridge of the forming crater rim. This regime of $(E/U_0)/n$ is generally accessed experimentally by clusters with thousands of atoms and results in the smallest yields. For the molecular systems, there is little or no molecular fragmentation. The simulations indicate, however, that the representation which includes U_0 as the only material property cannot be completely universal, because there are other material properties which influence the sputtering efficiency. Furthermore, neither the Y/n nor $Y/(E/U_0)$ representation includes the energy loss physics associated with molecular fragmentation in the high $(E/U_0)/n$ regime. The analysis of the universal concept implies for practical applications that if the objective of the experiment is large material removal, then the high energy per cluster atom regime is applicable. If the objective is little or no molecular fragmentation in organic materials, then the low energy per atom regime is appropriate.

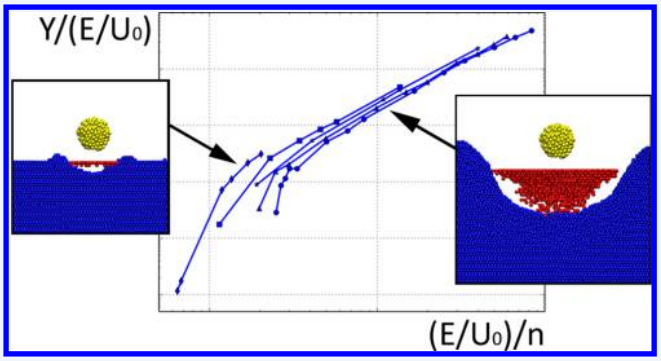

1. INTRODUCTION

The introduction of cluster beams in secondary-ion mass spectrometry (SIMS) has facilitated depth profiling and three-dimensional (3D) imaging of organic samples with high sensitivity and depth resolution.[1−3] In addition, there are enhanced high-mass sputtering yields of organic materials and reduced accumulation of damage. Recently, the noble gas cluster beams have become popular for these applications.[4,5] Chemical neutrality of the noble gases solves the problem of sample contamination due to chemical reactions between the projectile cluster and the sample material. The new applications of SIMS for organic material characterization has encouraged complementary theoretical studies to understand the basic events occurring in the cluster bombardment process. A characteristic measurement quantity in SIMS is the sputtering yield of material that is ejected per incident cluster. The yield is affected not only by the cluster composition, but also by the cluster size, energy, and impact angle. The issue is how to compare the data in an organized manner in order to

Received: March 30, 2015

DOI: 10.1021/acs.accounts.5b00303
Acc. Chem. Res. XXXX, XXX, XXX−XXX

understand common trends and help to optimize the experimental conditions. A thought-provoking observation was made that the spread in data points in the dependence of the sputtering yield Y versus initial cluster kinetic energy E can be reduced to nearly a curve if Y and E are expressed in quantities scaled by the number of atoms n in the cluster, that is, Y/n versus E/n.[6] The Y versus E dependence recast in terms of the scaled variables exhibits indications of universality, as the scaled yields for different sputtering conditions are close to falling on the same curve.

Universal descriptions of physical processes are commonly used in science. They allow for a simplification of the description of different (but similar) systems, determination of the common behavior and general properties, and have practical applications. A classic example is the Principle of Corresponding States (PCS), proposed by van der Waals in the 19th century for the description of noble gases and certain liquids. The PCS results in a universal equation of states with dimensionless scaled variables. The useful application of the PCS is calculation of thermodynamic correlations, an example of which is the Z-factor chart of Standing and Katz,[7] where the compressibility factor Z is plotted as a function of the scaled pressure. In general, the compressibility factors of gases with the same scaled temperature fall on the same curve. These correlations have been valuable in development of models to predict thermodynamic properties of liquids. Such predictive models are alternatives to the experimental measurements that can be expensive and time-consuming. Therefore, since the Y versus E dependence for cluster bombardment can be recast in the form that appears to exhibit universality, there is seduction to find a universal description for the cluster sputtering process, which would result in formulation of a predictive model of sputtering with possible practical applications for optimizing SIMS experiments.

The reduced spread in data points for the Y/n versus E/n dependence was observed in numerous studies, both experimental[8−10] and computational,[6,11−13] for a variety of solids sputtered by cluster beams (C_{60}, Ar_n), starting from atomic solids (Ag, Au, Si), through simple compounds (SiO_2) to organic molecular and polymeric solids (octane, Irganox, polystyrene). Representative results are shown in Figure 1. The dependence obtained from molecular dynamics (MD) simulations of Ar_n cluster bombardment of an amorphous Ar solid[6] and for experimental measurements of Ar_n cluster bombardment of atomic and organic solids[10] are shown in Figure 1a and b, respectively. For atomic solids, the yields are given in number of ejected atoms. For consistency, for organic solids, the yields are given in volume units (nm^3) per volume of a cube of side 0.27 nm, which is the average volume occupied by either a C, O, or N atom in the organic solids when the H atoms are ignored.[10] We will use the name "atomic equivalent" for this unit of the yield and denote the yields given in either atoms or atomic equivalents by Y_{at}. The dependence is plotted on a log−log scale to facilitate comparison between values that differ by many orders of magnitude. The yields for Ar self-sputtering are 100−1000 times larger than the yields for the other atomic solids (Au, Si). This disparity is a consequence of the difference between binding energies of the solids, namely, 0.083 eV/atom for amorphous Ar solid[6] versus ∼4 eV/atom for the other atomic solids.[10] As apparent in Figure 1b, the results for organic and atomic solids are similar in shape but separate into two regions that differ by orders of magnitude in value of the scaled yield. As suggested previously,[10] the yields for organic solids are larger than the yields for atomic solids, because many atoms can be ejected in a molecule or a polymer fragment at an energy cost much less than removing one atom from the atomic solid.

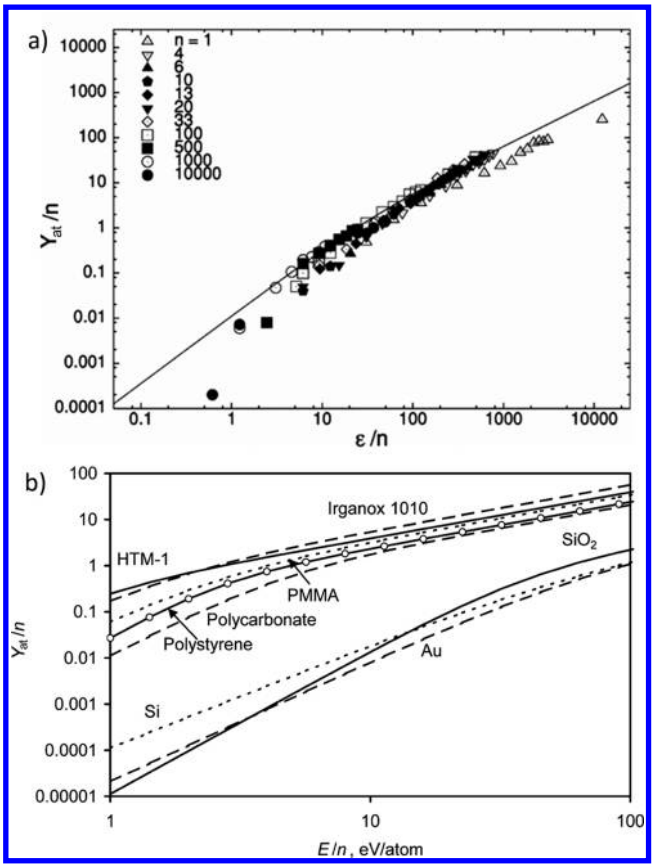

Figure 1. Sputtering yield in atoms (for atomic solids) or atomic equivalents (for molecular solids) per projectile atom Y_{at}/n versus energy per projectile atom E/n, for Ar_n cluster bombardment of (a) an amorphous atomic Ar solid from MD simulations and (b) atomic and molecular solids from experimental data. In panel (a), the variable ε denotes the energy scaled by the target binding energy of 0.083 eV, and therefore, the abscissa in eV per atom units can be obtained by shifting the scale by approximately an order of magnitude to the right.[6] Panel (a) adapted with permission from ref 6. Copyright 2004 The American Physical Society. Panel (b) adapted with permission from ref 10. Copyright 2013 American Chemical Society. Specifically, the ordinate axis label has been changed to Y_{at}/n in order to be consistent with the notation in this paper.

The curves shown in Figure 1 are results of fitting empirical equations to the data points.[6,10] There are different variations of empirical equations reported in the papers on Ar_n cluster bombardment of solids.[6,10,14,15] These equations usually employ a fitting parameter that can be associated with the binding energy of the solid and allow for extrapolation of the yields from a limited set of data for certain operational conditions. This approach does not, however, address the question of the physics that underlies the apparent universal dependence. In addition, lack of the convergence of the data points between organic and atomic solids does not support the concept of universality.

In our previous Letter on this topic,[16,17] we demonstrated that the convergence of the data points between molecular and atomic solids can be improved if the binding energy of the solid is explicitly included in the scaled variables and the yields are

DOI: 10.1021/acs.accounts.5b00303
Acc. Chem. Res. XXXX, XXX, XXX−XXX

given in consistent units. This study was based on MD simulations of Ar_n cluster bombardment of atomic Ag(111) and molecular octane solids. The previous results are first shown in Figure 2a in the form that is comparable with the experimental

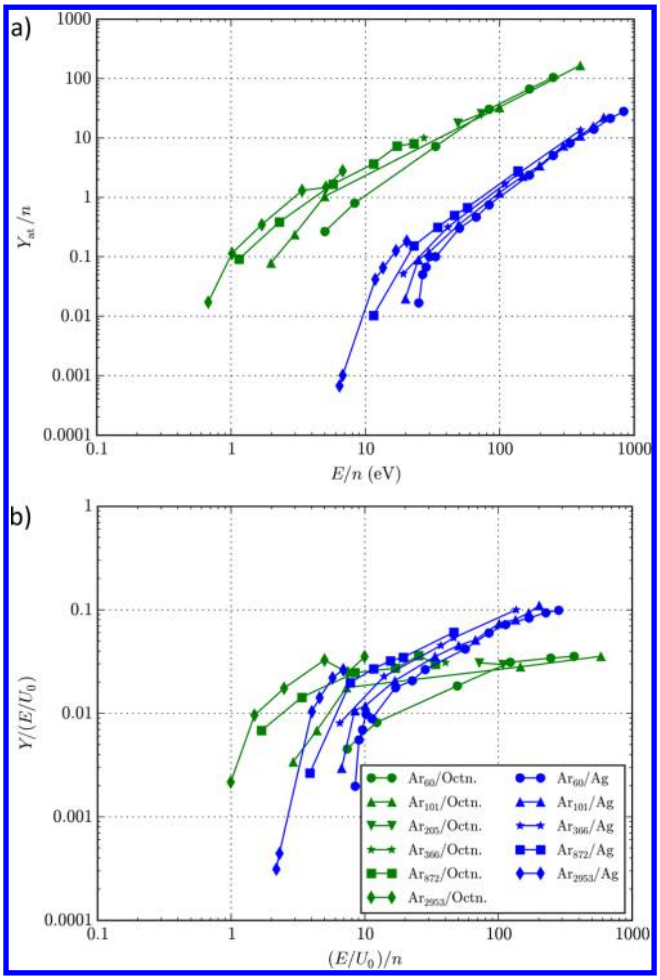

Figure 2. (a) Y_{at}/n versus E/n dependence with the sputtering yield in atoms (for Ag) and atomic equivalents (for octane) from MD simulations of Ar_n cluster bombardment of Ag(111) and octane solids. (b) $Y/(E/U_0)$ versus $(E/U_0)/n$ dependence for the same data with the yield in basic units of material, that is, in atoms (for Ag) and molecular equivalents (for octane). The figure adapted with permission from a previous work, refs 16 and 17. Copyright 2014 American Chemical Society.

results shown in Figure 1b, that is, Y_{at}/n versus E/n. Of note is that the curves in Figure 2 are composed from straight lines connecting the data points, as a guide to the eye, and are not a fit to an empirical equation. When viewing the data shown in Figures 1b and 2a, it is noticeable that in both data sets the Y_{at}/n values for organic solids increase from ~0.1 to ~10 atomic equivalents in the E/n range from ~1 to ~100 eV. The yields for atomic solids are 100−1000 times smaller in this E/n range. This comparison indicates that our computational results exhibit the same trends and are in semiquantitative agreement with the experimental values. We believe, therefore, it is justified to make conclusions applicable to the experiment based on the MD simulation results. The data from Figure 2a is next plotted in Figure 2b as $Y/(E/U_0)$ versus $(E/U_0)/n$, where U_0 is the binding energy of the solid.[16,17] To arrive at this form of the scaled representation, first n in the Y/n variable was replaced by E, because for a given (that is, fixed) E/n value, the number of cluster atoms n is proportional to the total cluster energy E. This change is justified because the total energy E is the primary factor that induces sputter ejection, not the cluster size n. Second, following others,[6,18,19] the initial energy E was scaled by the binding energy of the solid U_0. As a material property, the quantity U_0 is defined per basic unit of material, which is an atom for atomic solids and a molecule for molecular solids. The values of U_0 for the solids investigated are listed in the next section. Analogously, the quantity Y is given in atoms for atomic solids and in molecules for molecular solids. For molecular solids, however, to describe the sputtering process correctly in the high $(E/U_0)/n$ regime, where the contribution of intact molecules to the total sputtering yield is reduced due to molecular fragmentation, the quantity Y has to be given in molecular equivalents and the effect of molecular fragmentation described as a separate process. The number of sputtered molecular equivalents is calculated as the total sputtered mass divided by the mass of a molecule. We will use the symbol Y to denote the yield given in the basic unit of material, that is, in atoms and molecular equivalents for atomic and molecular solids, respectively. As apparent in Figure 2b, there is a noticeable improvement in data convergence between atomic and molecular solids over Figure 2a. All scaled yield values agree within an order of magnitude of each other. The high $(E/U_0)/n$ portion of the curves for octane is, however, flatter than for Ag. This trend, which is also seen experimentally as shown in Figure 1b, is associated with a portion of the incident energy being consumed by molecular fragmentation and internal excitation of ejected species in the high $(E/U_0)/n$ regime and will be discussed in the next section in greater detail.

The goal of the study presented in this Account is to elucidate the physical foundation of the apparent universal dependence of the sputtering yield on initial cluster energy and cluster size by means of molecular dynamics simulation. The protocol includes investigation of the properties of various solids under cluster bombardment in order to identify the common behavior and underlying mechanisms of ejection. Molecular dynamics simulation is well suited for this purpose because it provides a mechanistic view of the modeled processes and allows for calculation of the parameters that are directly comparable with experimental values. The description of the computational methods were given elsewhere.[20−23] Of note is that we employed atomistic models of organic materials to properly model molecular fragmentation and internal excitation. These calculations are excessively time and computing resources consuming.[21,23] Therefore, for some substrates, especially β-carotene, a limited number of beam conditions have been calculated to confirm the observed trends. In this study, we will focus on Ar clusters, which are popular beam sources for molecular SIMS, impinging at normal incidence to determine the most characteristic features of noble gas cluster bombardment.

2. EXPLORATION OF UNIVERSALITY VIA THE MECHANISMS OF SPUTTERING

The data given in Figure 2b for Ag and octane (C_8H_{18}) have been supplemented with results from simulations of Ar_n cluster bombardment of the two molecular solids, benzene (C_6H_6) and β-carotene ($C_{40}H_{56}$), as shown in Figure 3. The octane molecule (n-octane isomer) is a linear saturated hydrocarbon approximately 0.9 nm long. The molecule of β-carotene is an unsaturated linear hydrocarbon, approximately 2.9 nm long,

DOI: 10.1021/acs.accounts.5b00303
Acc. Chem. Res. XXXX, XXX, XXX−XXX

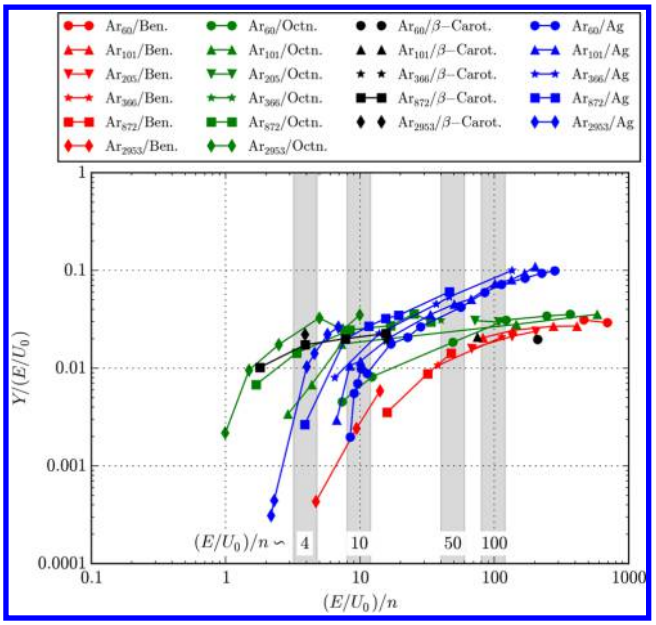

Figure 3. Yield in atoms (Ag) or molecular equivalents (molecular solids) per scaled energy $Y/(E/U_0)$ versus scaled energy per projectile atom $(E/U_0)/n$ for simulations of Ar_n cluster bombardment of Ag(111) and molecular (benzene, octane, and β-carotene) solids. The shaded rectangles mark the bands of $(E/U_0)/n$ around the values of 4, 10, 50, and 100.

with two rings at both ends of the chain. The benzene molecule is an aromatic (ring-shaped) hydrocarbon with the diameter of approximately 0.3 nm. For comparison, the diameters of the argon clusters range from 1.4 nm for Ar_{60}, through 2.8 nm for Ar_{366}, to 5.6 nm for Ar_{2953}. The binding energies U_0, as calculated from interaction potentials used in the simulations, for benzene, octane, β-carotene, and Ag solids are 0.36, 0.68, 1.91, and 2.95 eV per molecule or atom (Ag), respectively. Of note is that the conditions for the simulations were chosen before we understood that the appropriate quantity for the abscissa is the scaled energy per projectile atom $(E/U_0)/n$, and thus the data points are not all aligned at the same $(E/U_0)/n$ values.

Overall, the new results fit the previously described trends.[16,17] All four systems have scaled yield curves similar to each other with a linear part in the high $(E/U_0)/n$ regime and a curved part in the low $(E/U_0)/n$ regime. We used snapshots from the simulation to identify characteristics of each of the $(E/U_0)/n$ regimes. Four bands of scaled energy per projectile atom, $(E/U_0)/n \sim 4$, 10, 50, and 100, were chosen for analysis. In addition, the total energy E values were chosen from the experimentally accessible range, approximately 5−40 keV. Shown in Figures 4 and 5 are snapshots from the simulations to be used for discussion of the sputtering mechanisms.

Examining first the four snapshots from the simulations on the Ag system (Figure 4a−d), there is a change in the ejection mechanism visible with the change of the $(E/U_0)/n$ values. For $(E/U_0)/n \sim 100$ and an experimentally accessible projectile kinetic energy E, the clusters are typically composed of tens of atoms to a hundred of atoms, as shown in Figure 4d for Ar_{101} at 40 keV. The mechanism of emission was described previously by the mesoscale energy deposition footprint model (MEDF) for C_{60} cluster bombardment.[19] The cluster impacts the surface and deposits ∼90% of its energy in ∼100 fs in a few nm in the near surface region of the solid. This quick energy deposition process is possible because the large energy per atom in the cluster enables the cluster to penetrate the sample material into the bulk. The energized volume then induces a fluid flow and an approximately cone-shaped volume of the sample is ejected, as shown in Animation 1. The conical volume of emission is

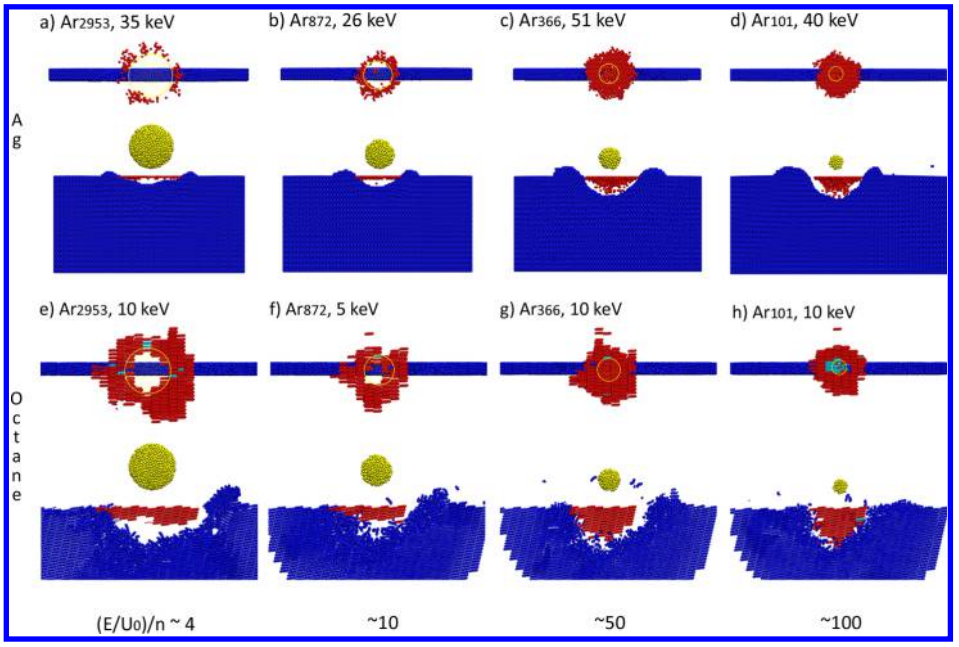

Figure 4. Top and side-sectional views for Ar_n cluster bombardment of (a−d) Ag(111) and (e−h) octane solids. Cluster sizes and initial kinetic energies are given in the figure. The results for the same $(E/U_0)/n$ values are vertically aligned. The cluster atoms (yellow) are shown at their original positions and an outline of the cluster is shown in the top view. The atoms and molecules that remain in the sample and are within a 1.5 nm slice centered at the aiming point of the projectile cluster are shown in blue at their final positions. All of the ejected Ag atoms or intact octane molecules (red), and molecular fragments (cyan) are shown at their original positions in the sample.

DOI: 10.1021/acs.accounts.5b00303
Acc. Chem. Res. XXXX, XXX, XXX−XXX

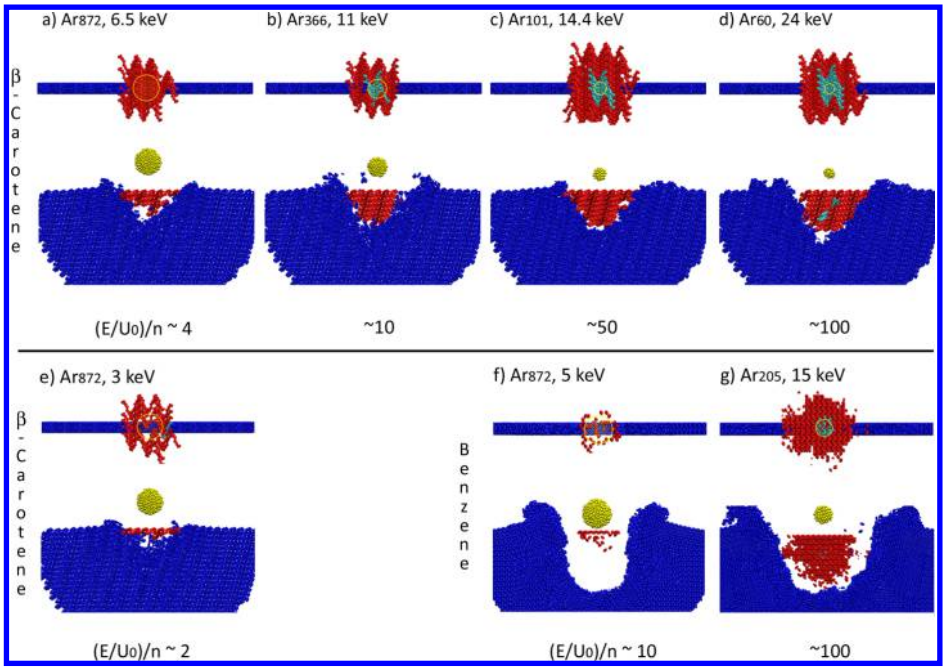

Figure 5. Snapshots for Ar_n cluster bombardment of (a–e) β-carotene and (f–g) benzene solids. β-Carotene results are given for the $(E/U_0)/n$ values in the range from 2 to 100, and benzene results are given for two $(E/U_0)/n$ values, 10 and 100. Refer to Figure 4 caption for description of the coloring scheme.

predicted by the MEDF model. This mechanism is typical for the near-linear region of the log–log plot, including $(E/U_0)/n \geq \sim 70$ for benzene, $\geq \sim 40$ for Ag(111) and octane, and $\geq \sim 10$ for β-carotene, as shown in Figure 3.

For the low $(E/U_0)/n$ regime ($\leq \sim 40$ for benzene, $\leq \sim 20$ for Ag(111) and octane, and $\leq \sim 2$ for β-carotene) and an experimentally accessible E, the clusters are typically thousands of atoms, as shown in Figure 4a for Ar_{2953} at 35 keV. In this case, the cluster deforms the surface pushing up material around the edge of the cluster and ejecting particles from a ring-shaped ridge of the forming crater rim, as shown in Animation 2. The energy per cluster atom is not sufficient for the cluster to penetrate into the bulk of the sample and the energy deposition process is relatively slow. This kind of the ejection mechanism has been previously described for organic solids irradiated at normal incidence by big clusters as the cluster blocking effect.[21,24] This effect manifests itself by material ejection at large polar angles, so-called lateral sputtering.[25] Snapshots at intermediate $(E/U_0)/n$ values (Figure 4b and c) show that there is a continuous transition from one mechanism to the other. As $(E/U_0)/n$ decreases, the conical region of emission is thinning and the emerging cluster blocking effect imposes the ring-shaped volume of emission.

As noted above, the high $(E/U_0)/n$ regime is described by the MEDF model and exhibits the conical volume of emission. In this regime, there is the highest level of convergence of the $Y/(E/U_0)$ values for a given data set, as shown in Figure 3. This property indicates that for a given $(E/U_0)/n$ value, the yield Y, which value is directly related to the volume of the ejected material, is roughly proportional to the scaled energy E/U_0 or, equivalently, to the cluster size n. This regime results in the largest total yields. Conversely, in the low $(E/U_0)/n$ regime, which exhibits irregular ring-shaped volume of emission, the $Y/(E/U_0)$ values vary up to almost two orders of magnitude, which indicates that for a given $(E/U_0)/n$ value the yield Y highly and disproportionately depends on the scaled energy E/U_0 or, equivalently, on the cluster size n. This regime results in the smallest total yields.

In order to support the concept of universality, the mechanism of sputtering for a molecular system should be similar to that for an atomic system at the same scaled energy per atom $(E/U_0)/n$ values. The snapshots from four simulations of the octane sample, shown in Figures 4e–h, in fact exhibit the same qualitative views as for Ag. At the largest $(E/U_0)/n$ value, there is a conical volume of emission. As $(E/U_0)/n$ decreases, the emission volume gets less deep and at the smallest two $(E/U_0)/n$ values the ring-shaped emission volume is visible. A representative case with $(E/U_0)/n \sim 10$ is shown in Animation 3. Not only do the two systems, Ag and octane, exhibit the same trend in ejection mechanisms, but the transition in mechanisms occurs at similar scaled energy per projectile atom $(E/U_0)/n$ values. The observed similarities in the ejection mechanism between the two solids, molecular and atomic, support the statement of universality.

The simulations indicate, however, that the representation of $Y/(E/U_0)$ versus $(E/U_0)/n$, which includes U_0 as the only material property cannot be completely universal, because there are other material properties and physical processes which influence the sputtering efficiency. We have demonstrated that there is an effect of material properties on the general trend in the previous Letter,[16,17] by comparing the results of Ar_n cluster bombardment of an Al(111) solid with the results for Ag(111), Au(111), and Pt(111) solids. The current results for benzene and β-carotene when compared with the octane results enrich this observation. As apparent in Figure 3, the values of the scaled yield $Y/(E/U_0)$ fall off faster as $(E/U_0)/n$ decreases for the benzene solid than for the other two molecular systems. The benzene solid exhibits a typical conical volume of emission and ring-shaped emission volume for large and small values of $(E/U_0)/n$, respectively, as shown in Figure 5f and g for two representative cases. There is, however, a larger crater and rim formed if compared to the other two molecular solids for the

DOI: 10.1021/acs.accounts.5b00303
Acc. Chem. Res. XXXX, XXX, XXX–XXX

same $(E/U_0)/n$ values. The dynamics of this process is shown in Animation 5 for conditions with $(E/U_0)/n \sim 10$. Due to the small size and ringlike shape of the benzene molecules, they can easily be relocated in the crater region.[21,24,26] Consequently, the final crater is much larger than the ejected volume of molecules and a significant portion of material is moved forming much larger rim than the rims seen in Figure 4e−h for octane and in Figure 5a−e for β-carotene. The energy which is consumed by the extensive material displacement reduces the fraction of the total energy E that can be utilized for sputtering. For comparison, in the octane solid with the same $(E/U_0)/n$, as shown in Animation 3, only a small rim is formed, and the ejected volume nearly fills the vacated crater. This characteristic of the octane solid is due to its structure composed of closely packed elongated molecules, where there is minimal displacement of material possible within the bulk and molecular relocation occurs mainly along the edges of the forming crater.[20] The last system to examine is β-carotene. As apparent in Figure 3, this system does not exhibit as much of a falloff of the $Y/(E/U_0)$ values as $(E/U_0)/n$ decreases as benzene, octane, and Ag do. Snapshots from five simulations on the β-carotene system are shown in Figure 5a−e. The general mechanistic trend is present; namely, the conical volume of emission is getting less deep and transitions into the ring-shaped volume as $(E/U_0)/n$ is decreasing. However, the appearance of the ring-shaped emission volume is not reached until $(E/U_0)/n$ drops below 2. For the value of $(E/U_0)/n \sim 4$, the volume of emission in the β-carotene system is still deep and the ring-shaped emission region is not yet present, although it is present in the octane system, as visible in Figure 4e. The material motion for the β-carotene system is distinct. In contrast to octane, the β-carotene solid consists of molecules intertwined with each other. In this crisscrossed system the atoms of the Ar cluster tend to sweep away the molecules they interact with resulting in deeper volume of emission, as shown in Animation 4.

As noted before, there is a flattening of the scaled yield $Y/(E/U_0)$ curves for molecular solids in the high $(E/U_0)/n$ regime when compared to Ag(111). Figure 6 shows the yield of molecular fragments given in molecular equivalents of ejected mass as a percentage of the total yield Y. For β-carotene the molecular fragmentation is largest because the molecules are relatively long and intertwined, and as such easy to fragment by the incident cluster.[27] The percentage of fragmented molecules increases rapidly for $(E/U_0)/n > \sim 10$, and reaches approximately 30−40% of Y for $(E/U_0)/n > \sim 100$. For octane and benzene the percentage of fragmented molecules is smaller, ranging up to approximately 13% of Y for $(E/U_0)/n > \sim 100$. Similar trends are reported in other experimental and simulation studies.[11,28] The original positions of the fragmented molecules tend to be directly under the impact point of the incident cluster, where the density of deposited energy is the largest.[20] The fragmented molecules are shown in cyan in Figures 4 and 5 at their original positions. The fragmentation process, which utilizes energy of 3−4 eV per bond cleavage in these hydrocarbon systems, consumes a portion of the total energy E and reduces the fraction that can be utilized for sputtering. The third process, which we identified as consuming a significant portion of the total energy E in the high $(E/U_0)/n$ regime, is ejection of molecules and molecular fragments with large internal energy. Although a true description of energy transfer to vibrational modes should involve quantum mechanics, we approximate from the classical simulations the percentage of the total energy E that is consumed by the

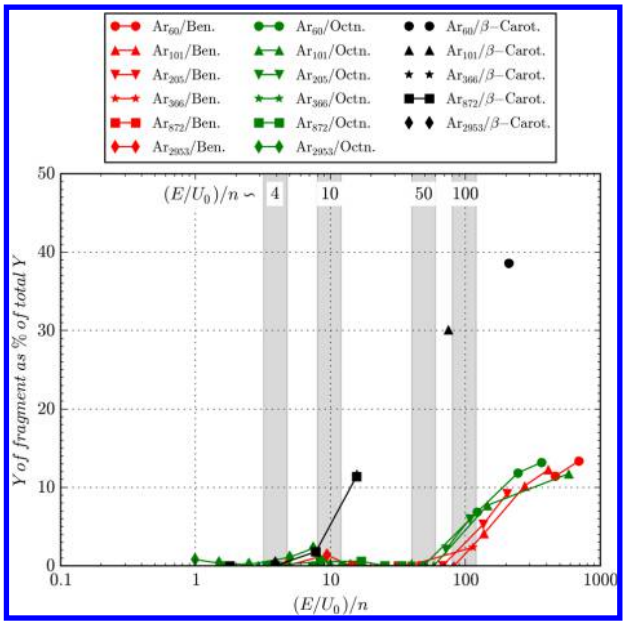

Figure 6. Yield of fragments in molecular equivalents of ejected mass as percentage of the total yield versus scaled energy per projectile atom $(E/U_0)/n$ for simulations of Ar_n cluster bombardment of molecular solids (benzene, octane, and β-carotene). The shaded rectangles mark the bands of $(E/U_0)/n$ around the values of 4, 10, 50, and 100.

internal excitation to be for $(E/U_0)/n > \sim 100$: 40% for β-carotene (linear molecules containing the largest number of atoms, as such capable of accumulating the largest amount of internal energy), 32% for octane, and 24% for benzene (stiff-ring-shaped molecules with the smallest number of atoms). The reason for the $Y/(E/U_0)$ versus $(E/U_0)/n$ dependence flattening in the high $(E/U_0)/n$ regime is redistribution of a fraction of E into processes other than sputtering, thus reducing the sputtering yields. These processes include molecular fragmentation, ejection of molecules and molecular fragments with large internal energy and material relocation in the solid. For the β-carotene system, the $Y/(E/U_0)$ values in the high $(E/U_0)/n$ regime are the smallest among all the systems, because the yield is reduced by the largest effects of fragmentation and internal excitation. To confirm this trend, we show one data point for Ar_{60} bombardment in Figure 3. For octane and benzene, the intensity of the fragmentation effect is similar in both systems; however, the smallest rate of internal excitation for benzene is overbalanced by the process of extensive material relocation. As a result, the $Y/(E/U_0)$ values in the high $(E/U_0)/n$ regime are smaller for benzene than for octane.

The challenge for understanding all experimental conditions is that, in principle, any cluster size n and any energy E can be chosen, giving a matrix of choices. The trends in mechanisms persist, however. For a constant E and varying n, small clusters have large $(E/U_0)/n$ values and tend to exhibit the conical volume of ejection, whereas large clusters have small $(E/U_0)/n$ values and tend to exhibit the ring-shaped volume of ejection. For constant n and varying E, small energies induce ejection from a ringlike volume, while large energies induce ejection from a conical volume. Interestingly, when the value of $(E/U_0)/n$ is fixed by varying proportionately both E and n at a time, the sputtering mechanism also transitions from the ringlike type of ejection to conical type of ejection, as the total energy of the cluster E increases. This qualitative change of the sputtering mechanism for a given $(E/U_0)/n$ value is the basis of the

DOI: 10.1021/acs.accounts.5b00303
Acc. Chem. Res. XXXX, XXX, XXX−XXX

described previously synergistic cluster effect.[16,17] This effect manifests itself in the way that a larger cluster induces a larger yield than the yield that would increase just proportionately to the cluster total energy E or, equivalently, the cluster size n.

3. APPLICATION TO EXPERIMENTAL RESULTS

Recent experimental studies of positive secondary-ion emission from model biocompounds under Ar_n cluster bombardment over a range of cluster sizes n and energies E show consistently that the useful molecular ion yield maximizes or plateaus in the region of $E/n \geq 10$ eV and drops rapidly below this value of E/n.[28,29] As shown in Figure 3 and explained above, the plateauing of the yield of organic material will eventually occur as the energy per cluster atom increases, because other processes are induced that reduce the yield. Moreover, the contribution of the molecular yield to the total yield is reduced by increasing molecular fragmentation, as shown in Figure 6. The high energy per atom regime, however, results in largest total yields and as such is appropriate if large material removal is the objective of the experiment. The experimental observation that the ion yield drops rapidly below the critical value of E/n coincides with the fact, as shown in Figure 6, that the fragmentation rate drops eventually to nearly zero as $(E/U_0)/n$ decreases. The total yields, however, remain relatively constant around the critical values of $(E/U_0)/n$, as apparent in Figure 3. If the ionization process, likewise the fragmentation process, is associated with some energetic events, the logical conclusion is that there is much more molecular signal below $E/n = 10$ eV than what is being measured experimentally in the ion signal. Methods to increase the number of ions in the low E/n regime are therefore needed.

4. SUMMARY

The apparent universal dependence of the sputtering yield on the projectile cluster energy is based on similarities in ejection mechanisms and changing trends for molecular and atomic solids if the binding energy of the solid is explicitly included in the scaled variables and the yield is given in consistent units. The limitations of this approach come from the fact that all the material properties of the solid and other processes that influence the sputtering efficiency cannot be solely described by the binding energy. The analysis of the physical foundation of the universal concept explains the experimental observation of the organic yield plateauing in the high energy per cluster atom regime, and implies that there is a useful molecular signal in the low energy per atom regime, which is not detected because of not sufficient ionization.

■ ASSOCIATED CONTENT

Supporting Information

The Supporting Information is available free of charge on the ACS Publications website at DOI: 10.1021/acs.accounts.5b00303.

Animation 1 for 40 keV Ar_{101}/Ag(111), $(E/U_0)/n \sim 100$ (MPG)

Animation 2 for 26 keV Ar_{872}/Ag(111), $(E/U_0)/n \sim 10$ (MPG)

Animation 3 for 5 keV Ar_{872}/octane, $(E/U_0)/n \sim 10$ (MPG)

Animation 4 for 6.5 keV Ar_{872}/β-carotene, $(E/U_0)/n \sim 4$ (MPG)

Animation 5 for 5 keV Ar_{872}/benzene, $(E/U_0)/n \sim 10$ (MPG)

■ AUTHOR INFORMATION

Corresponding Author

*E-mail: rjp25@psu.edu.

Notes

The authors declare no competing financial interest.

Biographies

Robert J. Paruch received his Ph.D. in 2012 at the Jagiellonian University in Krakow, Poland. Currently he is a postdoctoral fellow at Penn State University, the Department of Chemistry. His research interests are in computer modeling of physical processes, and data analysis and visualization. His current research project focuses on modeling of depth profiling for secondary-ion mass spectrometry by means of molecular dynamics simulation and Python scripting.

Zbigniew Postawa received his Ph.D. in 1987 at the Jagiellonian University in Krakow, Poland. After a postdoctoral appointment at Penn State University, he joined the physics faculty of the Jagiellonian University in 1991, where he is currently Professor of Physics. He is interested in modeling interaction of cluster projectiles with solid surfaces with emphasis on processes important for secondary-ion mass spectrometry.

Barbara J. Garrison received her Ph.D. in 1975 at the University of California at Berkeley. She joined the chemistry faculty of Penn State University in 1979 where she is currently the Shapiro Professor of Chemistry and Head of the Department of Chemistry. She has long-standing interests in modeling fast energy deposition at surfaces including secondary-ion mass spectrometry and laser ablation with an emphasis on modeling phenomena that can be interfaced with experimental results.

■ ACKNOWLEDGMENTS

The authors gratefully acknowledge financial support from the National Science Foundation, Grant CHE-1212645, and the Polish National Science Center, Grant 2013/09/B/ST4/00094. We appreciate the support of the Penn State Institute for CyberScience in performing these simulations. The visualization of data presented in this paper was done with the matplotlib Python library[30] and the Visual Molecular Dynamics program.[31]

■ REFERENCES

(1) Winograd, N.; Garrison, B. J. Biological Cluster Mass Spectrometry. *Annu. Rev. Phys. Chem.* **2010**, *61*, 305−322.

(2) Winograd, N. The Magic of Cluster Sims. *Anal. Chem.* **2005**, *77*, 142A−149A.

(3) Mahoney, C. M. Cluster Secondary Ion Mass Spectrometry of Polymers and Related Materials. *Mass Spectrom. Rev.* **2010**, *29*, 247−293.

(4) Yamada, I.; Matsuo, J.; Toyoda, N.; Kirkpatrick, A. Materials Processing by Gas Cluster Ion Beams. *Mater. Sci. Eng., R* **2001**, *34*, 231−295.

(5) Shard, A. G.; Havelund, R.; Seah, M. P.; Spencer, S. J.; Gilmore, I. S.; Winograd, N.; Mao, D.; Miyayama, T.; Niehuis, E.; Rading, D.; Moellers, R. Argon Cluster Ion Beams for Organic Depth Profiling: Results from a Vamas Interlaboratory Study. *Anal. Chem.* **2012**, *84*, 7865−7873.

(6) Anders, C.; Urbassek, H. M.; Johnson, R. E. Linearity and Additivity in Cluster-Induced Sputtering: A Molecular-Dynamics

DOI: 10.1021/acs.accounts.5b00303
Acc. Chem. Res. XXXX, XXX, XXX−XXX

Study of van der Waals Bonded Systems. *Phys. Rev. B: Condens. Matter Mater. Phys.* **2004**, *70*, 155404.
(7) Standing, M. B.; Katz, D. L. Density of Natural Gases. *Trans. Soc. Pet. Eng.* **1942**, *146*, 140−149.
(8) Yang, L.; Seah, M. P.; Gilmore, I. S. Sputtering Yields for Gold Using Argon Gas Cluster Ion Beams. *J. Phys. Chem. C* **2012**, *116*, 23735−23741.
(9) Rading, D.; Moellers, R.; Cramer, H. G.; Niehuis, E. Dual Beam Depth Profiling of Polymer Materials: Comparison of C_{60} and Ar Cluster Ion Beams for Sputtering. *Surf. Interface Anal.* **2013**, *45*, 171−174.
(10) Seah, M. P. Universal Equation for Argon Gas Cluster Sputtering Yields. *J. Phys. Chem. C* **2013**, *117*, 12622−12632.
(11) Delcorte, A.; Garrison, B. J.; Hamraoui, K. Dynamics of Molecular Impacts on Soft Materials: From Fullerenes to Organic Nanodrops. *Anal. Chem.* **2009**, *81*, 6676−6686.
(12) Palka, G.; Rzeznik, L.; Paruch, R.; Postawa, Z. Molecular Dynamics Simulations of Energetic Ar Cluster Bombardment of Ag(111). *Acta Phys. Pol., A* **2013**, *123*, 831−833.
(13) Delcorte, A.; Cristaudo, V.; Lebec, V.; Czerwinski, B. Sputtering of Polymers by keV Clusters: Microscopic Views of the Molecular Dynamics. *Int. J. Mass Spectrom.* **2014**, *370*, 29−38.
(14) Seki, T.; Murase, T.; Matsuo, J. Cluster Size Dependence of Sputtering Yield by Cluster Ion Beam Irradiation. *Nucl. Instrum. Methods Phys. Res., Sect. B* **2006**, *242*, 179−181.
(15) Ichiki, K.; Ninomiya, S.; Seki, T.; Aoki, T.; Matsuo, J. Energy Effects on the Sputtering Yield of Si Bombarded with Gas Cluster Ion Beams. *AIP Conf. Proc.* **2011**, *1321*, 294−297.
(16) Paruch, R. J.; Garrison, B. J.; Mlynek, M.; Postawa, Z. On Universality in Sputtering Yields Due to Cluster Bombardment. *J. Phys. Chem. Lett.* **2014**, *5*, 3227−3230.
(17) Paruch, R. J.; Garrison, B. J.; Mlynek, M.; Postawa, Z. Correction to "on Universality in Sputtering Yields Due to Cluster Bombardment. *J. Phys. Chem. Lett.* **2014**, *5*, 3435−3435.
(18) Anders, C.; Urbassek, H. M. Effect of Binding Energy and Mass in Cluster-Induced Sputtering of van-der-Waals Bonded Systems. *Nucl. Instrum. Methods Phys. Res., Sect. B* **2005**, *228*, 84−91.
(19) Russo, M. F.; Garrison, B. J. Mesoscale Energy Deposition Footprint Model for Kiloelectronvolt Cluster Bombardment of Solids. *Anal. Chem.* **2006**, *78*, 7206−7210.
(20) Paruch, R. J.; Garrison, B. J.; Postawa, Z. Computed Molecular Depth Profile for C_{60} Bombardment of a Molecular Solid. *Anal. Chem.* **2013**, *85*, 11628−11633.
(21) Postawa, Z.; Paruch, R.; Rzeznik, L.; Garrison, B. J. Dynamics of Large Ar Cluster Bombardment of Organic Solids. *Surf. Interface Anal.* **2013**, *45*, 35−38.
(22) Paruch, R. J.; Postawa, Z.; Garrison, B. J. How Material Properties Affect Depth Profiles − Insight from Computer Modeling. *Surf. Interface Anal.* **2014**, *46*, 253−256.
(23) Palka, G.; Kanski, M.; Maciazek, D.; Garrison, B. J.; Postawa, Z. Computer Simulations of Material Ejection During C_{60} and Ar_m Bombardment of Octane and Beta-Carotene. *Nucl. Instrum. Methods Phys. Res., Sect. B* **2015**, *352*, 202−205.
(24) Czerwinski, B.; Rzeznik, L.; Paruch, R.; Garrison, B. J.; Postawa, Z. Effect of Impact Angle and Projectile Size on Sputtering Efficiency of Solid Benzene Investigated by Molecular Dynamics Simulations. *Nucl. Instrum. Methods Phys. Res., Sect. B* **2011**, *269*, 1578−1581.
(25) Insepov, Z.; Yamada, I. Molecular-Dynamics Simulation of Cluster Ion-Bombardment of Solid-Surfaces. *Nucl. Instrum. Methods Phys. Res., Sect. B* **1995**, *99*, 248−252.
(26) Rzeznik, L.; Paruch, R.; Garrison, B. J.; Postawa, Z. Sputtering of a Coarse-Grained Benzene and Ag(111) Crystals by Large Ar Clusters - Effect of Impact Angle and Cohesive Energy. *Surf. Interface Anal.* **2013**, *45*, 27−30.
(27) Postawa, Z.; Kanski, M.; Maciazek, D.; Paruch, R. J.; Garrison, B. J. Computer Simulations of Sputtering and Fragment Formation During keV C_{60} Bombardment of Octane and Beta-Carotene. *Surf. Interface Anal.* **2014**, *46*, 3−6.
(28) Gnaser, H.; Ichiki, K.; Matsuo, J. Sputtered Ion Emission under Size-Selected Ar_n^+ Cluster Ion Bombardment. *Surf. Interface Anal.* **2013**, *45*, 138−142.
(29) Sheraz née Rabbani, S.; Razo, I. B.; Kohn, T.; Lockyer, N. P.; Vickerman, J. C. Enhancing Ion Yields in Time-of-Flight-Secondary Ion Mass Spectrometry: A Comparative Study of Argon and Water Cluster Primary Beams. *Anal. Chem.* **2015**, *87*, 2367−2374.
(30) Hunter, J. D. Matplotlib: A 2D Graphics Environment. *Comput. Sci. Eng.* **2007**, *9*, 90−95.
(31) Humphrey, W.; Dalke, A.; Schulten, K. VMD: Visual Molecular Dynamics. *J. Mol. Graphics* **1996**, *14*, 33−38.

DOI: 10.1021/acs.accounts.5b00303
Acc. Chem. Res. XXXX, XXX, XXX−XXX